Imaging of Acute Head Emergencies

16

Majid Khan, Sneha Patel, and Ajay Singh

Introduction

In the management of acute intracranial emergencies, triage of patients is key, and therefore, the proper diagnosis on early imaging can go a long way in directing the appropriate workup and management.

Pseudo-subarachnoid Hemorrhage

Increased density in the subarachnoid spaces at the basal cisterns is typically seen in patients with diffuse subarachnoid hemorrhage. However, it is imperative to examine the brain parenchyma for signs of increased cerebral edema, as the increased density in the subarachnoid space may well be engorged dural, arterial, and venous vessels from brain swelling (Fig. 16.1). Other CT mimics of subarachnoid hemorrhage include intrathecal contrast injection, infectious meningitis, and leakage of intravascular contrast into the subarachnoid spaces.

The pathologic cause of the increased cisternal density is not definitively known, but is postulated to be secondary to a combination of factors, including displacement of normally hypodense cerebrospinal fluid, engorgement of the superficial vasculature, and the edematous and hypodense adjacent brain [1].

Carbon Monoxide Poisoning

Patients found unresponsive and brought for acute neuroimaging can have a whole host of imaging findings, some subtle and others obvious. Carbon monoxide poisoning is one potentially subtle imaging finding which, if detected early, can significantly improve the clinical prognosis of the patient.

Carbon monoxide poisoning is a typically symmetric anoxic encephalopathy, with a much higher affinity for hemoglobin than oxygen. Cerebral injury has a predilection for the globi pallidi (Fig. 16.2) [2]. The cerebral white matter may or may not be also involved, depending the duration of exposure. If diagnosed within 6 h on initial injury, long-term neuropsychiatric morbidity can be curtailed. Standard treatments include hyperbaric oxygen and 100 % oxygen.

Differential considerations include Creutzfeldt-Jakob disease, Wilson's disease, and Leigh syndrome, all entities which can affect the globi pallidi, although all of these have more widespread gray matter involvement than CO poisoning.

Central Nervous System Infections

Cerebral abscesses are typically located at the corticomedullary junction and have thin, regular capsule formation that appears hypointense on T2-weighted images. The causes of brain abscess include bacterial, fungal, or tuberculosis. The disease evolves from an early cerebritis and extensive T2 signal intensity abnormality to liquefaction and capsule formation.

The medial temporal lobe involvement by focal process can be from arterial ischemia, which originates from the PCA territory; pyogenic infection, which can arise from otogenic infection; and herpes encephalitis, which has a predilection

M. Khan, MD
Department of Radiology, Oakland University,
William Beaumont School of Medicine,
William Beaumont Hospital,
Royal Oak, MI, USA

S. Patel, MD
Department of Diagnostic Radiology,
William Beaumont Hospital,
Royal Oak, MI, USA

A. Singh, MD (✉)
Department of Radiology,
Massachusetts General Hospital, Harvard Medical School,
10 Museum Way, # 524, Boston, MA 02141, USA
e-mail: asingh1@partners.org

A. Singh (ed.), *Emergency Radiology*,
DOI 10.1007/978-1-4419-9592-6_16,

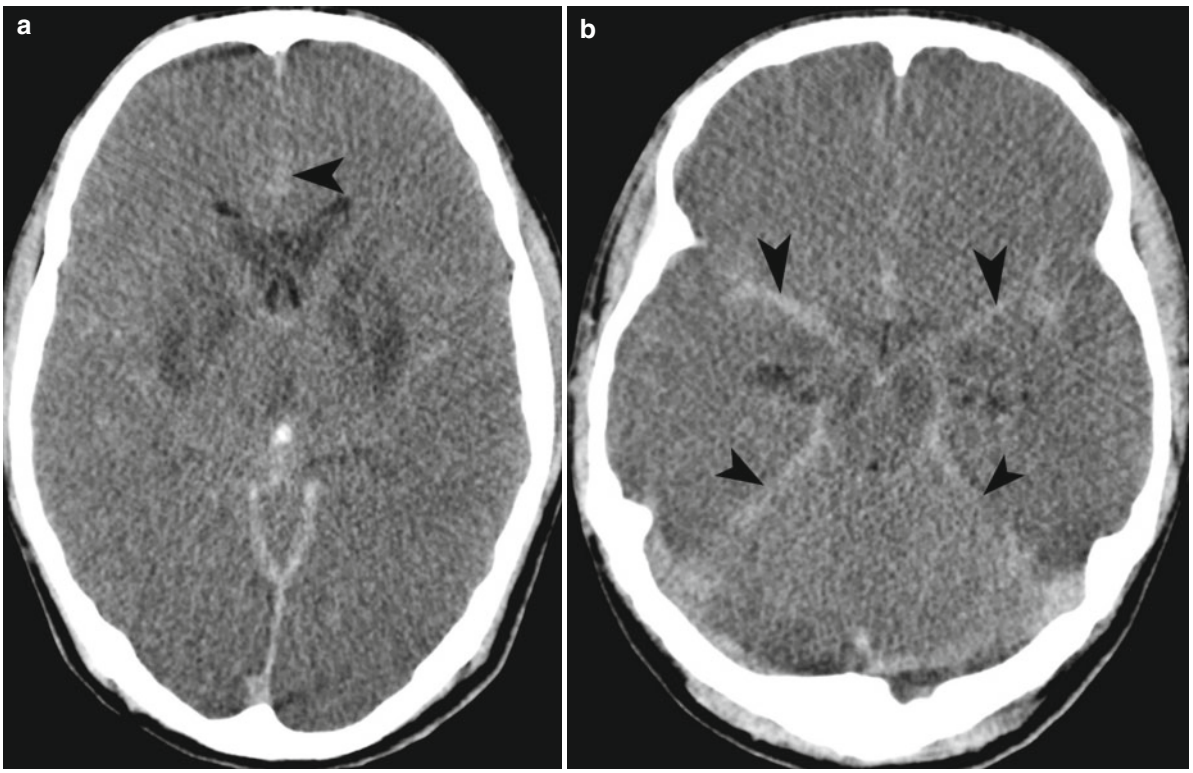

Fig. 16.1 (**a**, **b**) Cerebral edema. Noncontrast axial CT image of the brain shows diffuse hypodensity in the brain parenchyma, with loss of the gray-white interface compatible with brain edema. Extra-axial high attenuation (*arrowheads*) has the appearance of subarachnoid hemorrhage but is simply secondary to brain swelling

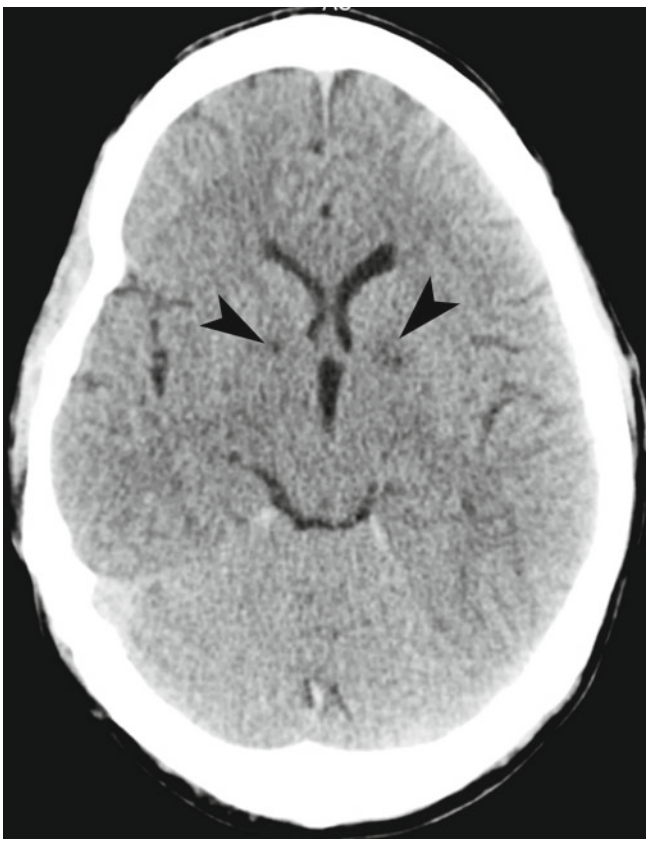

Fig. 16.2 Carbon monoxide poisoning. Noncontrast axial CT image of the brain shows subtle areas of decreased attenuation in bilateral globi pallidi (*arrowheads*), compatible with ischemic injury in the setting of carbon monoxide poisoning

for the hippocampal formation [3]. If the focal abnormality involves the lateral temporal lobe, MCA territory arterial ischemia should be considered. If the edema involves the entire temporal lobe, one has to consider tumor. If otogenic infection is left untreated, there can be dural breech, leading to empyema, cerebritis, and abscess formation (Fig. 16.3).

Parasitic infection, such as neurocysticercosis, paragonimiasis, and echinococcus infection, should be considered when there is history of travel to an endemic region. Neurocysticercosis is the most common parasitic infection involving the central nervous system in developing countries and is endemic to Mexico, South America, Africa, Eastern Europe, and Asia. The neurocysticercosis involving the central nervous system is of four types:

- Meningeal
- Parenchymal
- Ventricular
- Mixed

While the meningeal cysts form mostly in the basal meninges, parenchymal cysts are usually found in the

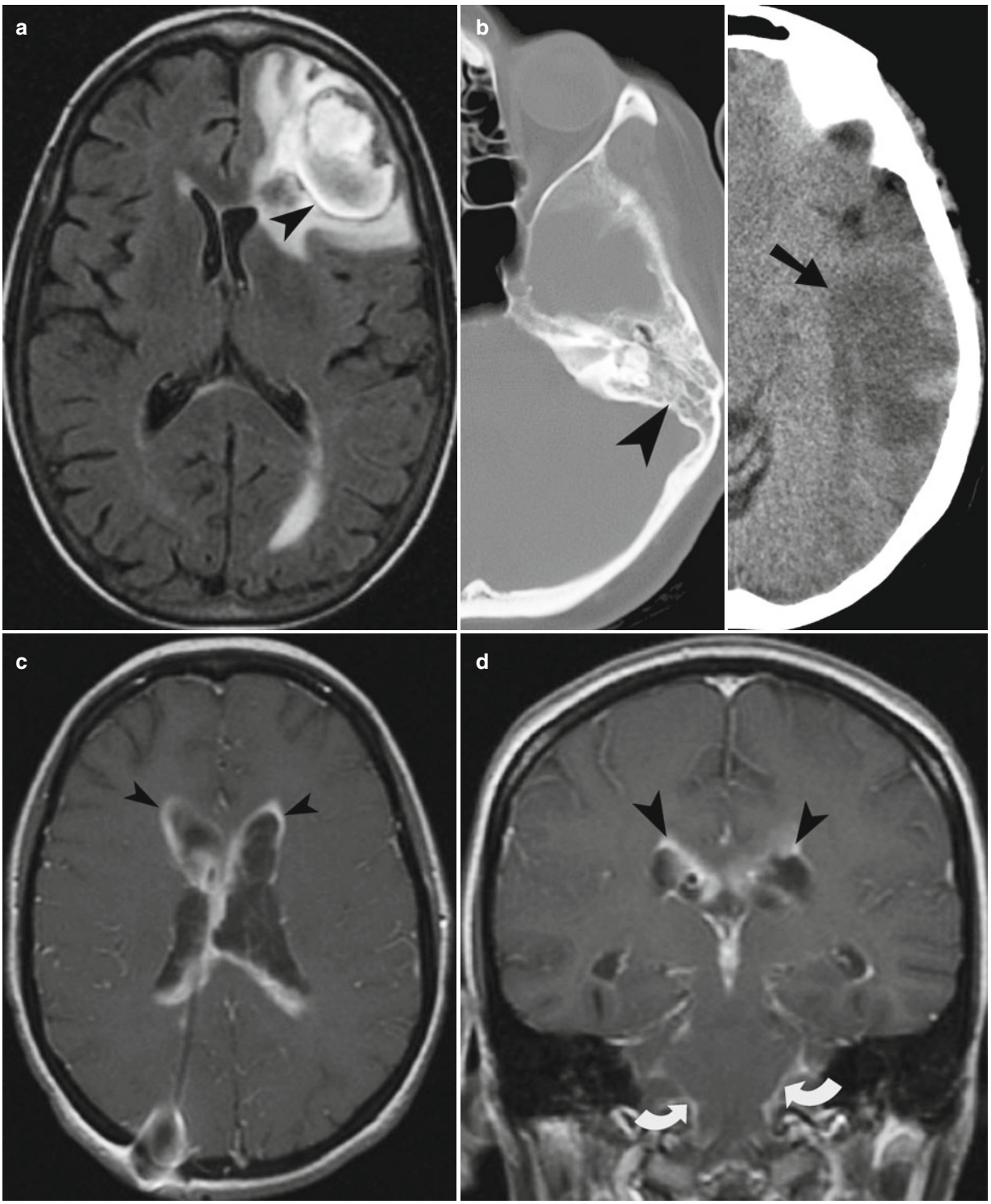

Fig. 16.3 Intracranial infection: brain abscess, ventriculitis, meningitis, and neurocysticercosis. (**a**) FLAIR sequence demonstrates left frontal brain abscess (*arrowhead*) from fungal infection with surrounding edema. The wall of the abscess is thinner on the medial aspect, a feature of brain abscess which is the result of limited vascular supply on the medial aspect. (**b**) Noncontrast axial CT image of the brain shows confluent decreased attenuation (*arrowhead*) in the left temporal lobe, from a combination of abscess and edema (*arrow*). Bone windows at the same level shows fluid in mastoid air cells (*arrowhead*). (**c**, **d**) Contrast-enhanced T1-weighted MRI shows extensive ependymal enhancement of the ventricular wall (*arrowheads*). There is also enhancement of the basal cisterns (*curved arrows*). The defect seen in the right parietal bone is from a ventriculostomy catheter which had become infected and was taken out. (**e**, **f**) T1-weighted sequence demonstrates multiple spherical parenchymal neurocysticercosis (*arrowheads*) containing scolex, at the gray-white matter junction. Postgadolinium T1-weighted (**f**) sequence shows rim enhancement of the multiple cystic lesions in the supratentorial compartment

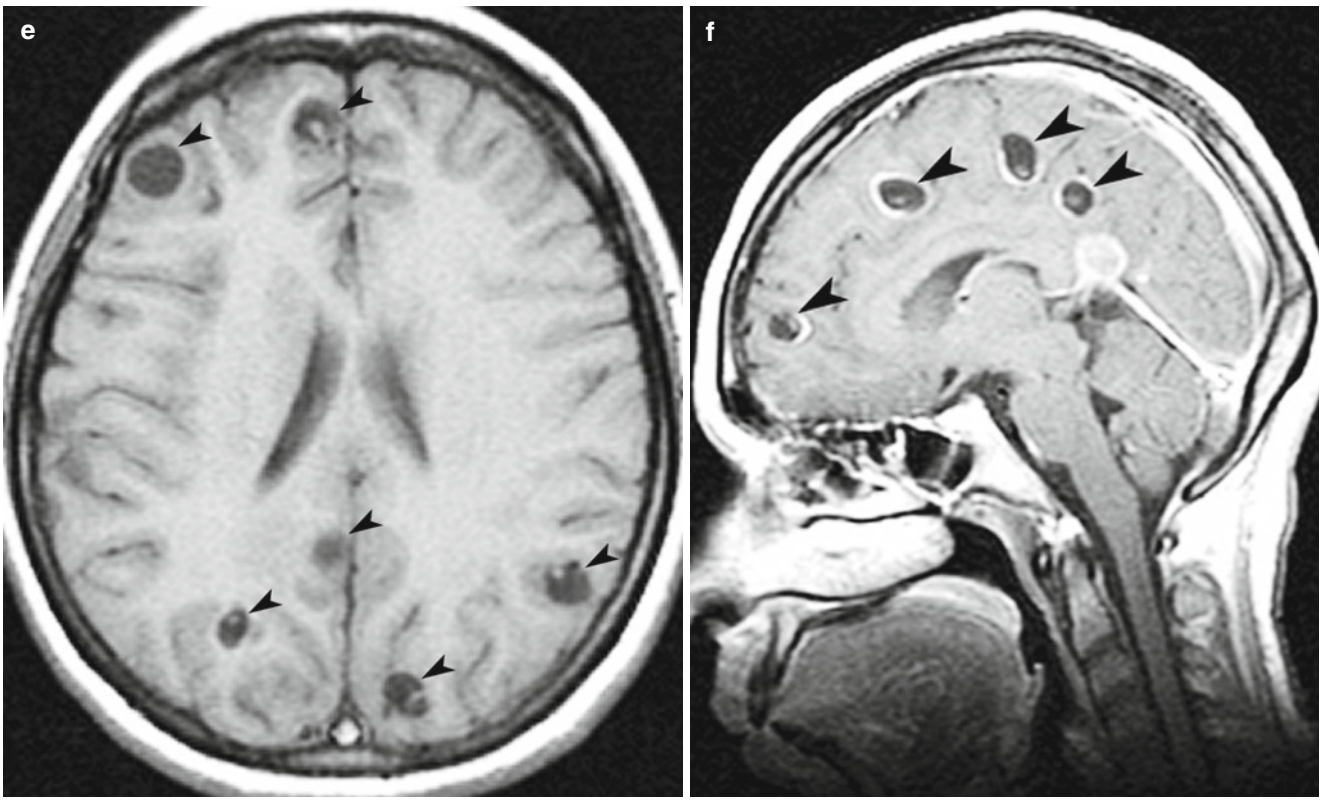

Fig. 16.3 (continued)

cerebral cortex. The white matter is rarely involved. Ventricular cysts are seen in 15 % of patients with neurocysticercosis, most commonly involving the fourth ventricle. In approximately nine fifths of cases of ventricular disease, there is associated parenchymal involvement.

Parenchymal neurocysticercosis is typically seen as 1 cm (range, 4–20 mm) diameter spherical shape lesion with a 2–3 mm mural nodule produced by the scolex. The presence of surrounding edema and enhancement of capsule indicates that the parasite is in degenerative or colloidal state. On T1-weighted sequence, the fluid in the cystic lesion is hypointense to white matter and hyperintense to cerebrospinal fluid. On T2-weighted sequence the cystic fluid is markedly hyperintense. There is usually no enhancement in the earlier vesicular stage, when the larva is still viable and the cyst is antigenically inert. In nodular calcified stage, cystic lesion is calcified and does not show any enhancement.

Herpes Encephalitis

Herpes simplex virus infection is ubiquitous in the general population, usually contracted initially via oronasopharyngeal contact. The virus then lies dormant within the trigeminal ganglion. HSV encephalitis is the most common viral infection in the central nervous system. What precipitates viral reactivation in the CNS is not known, although some patients have been found to have a viral prodrome prior to full manifestation [4]. Patients usually present with fever and a gradual onset of altered mental status, over the course of a few days. Infrequently are there focal neurological signs.

Fortunately, there are many imaging features for HSV encephalitis that are characteristic. The limbic system is a characteristic location (Fig. 16.4). It can be bilateral, usually asymmetric. Enhancement is typically gyriform. Restricted diffusion is often seen in the limbic system. Hemorrhage is a late feature. If a patient has these features, a presumptive diagnosis of herpes encephalitis should lead the clinical team to start IV acyclovir, as prompt antiviral therapy has been shown to improve outcomes.

The differential possibilities include infarction, especially if the symptoms are very acute in onset; postictal states can cause swelling and patchy areas of enhancements, mimicking HSV encephalitis, especially if the focus is in the temporal lobes, and limbic encephalitis, especially if the onset of symptoms is more gradual, such as over the course of months rather than days in herpetic encephalitis.

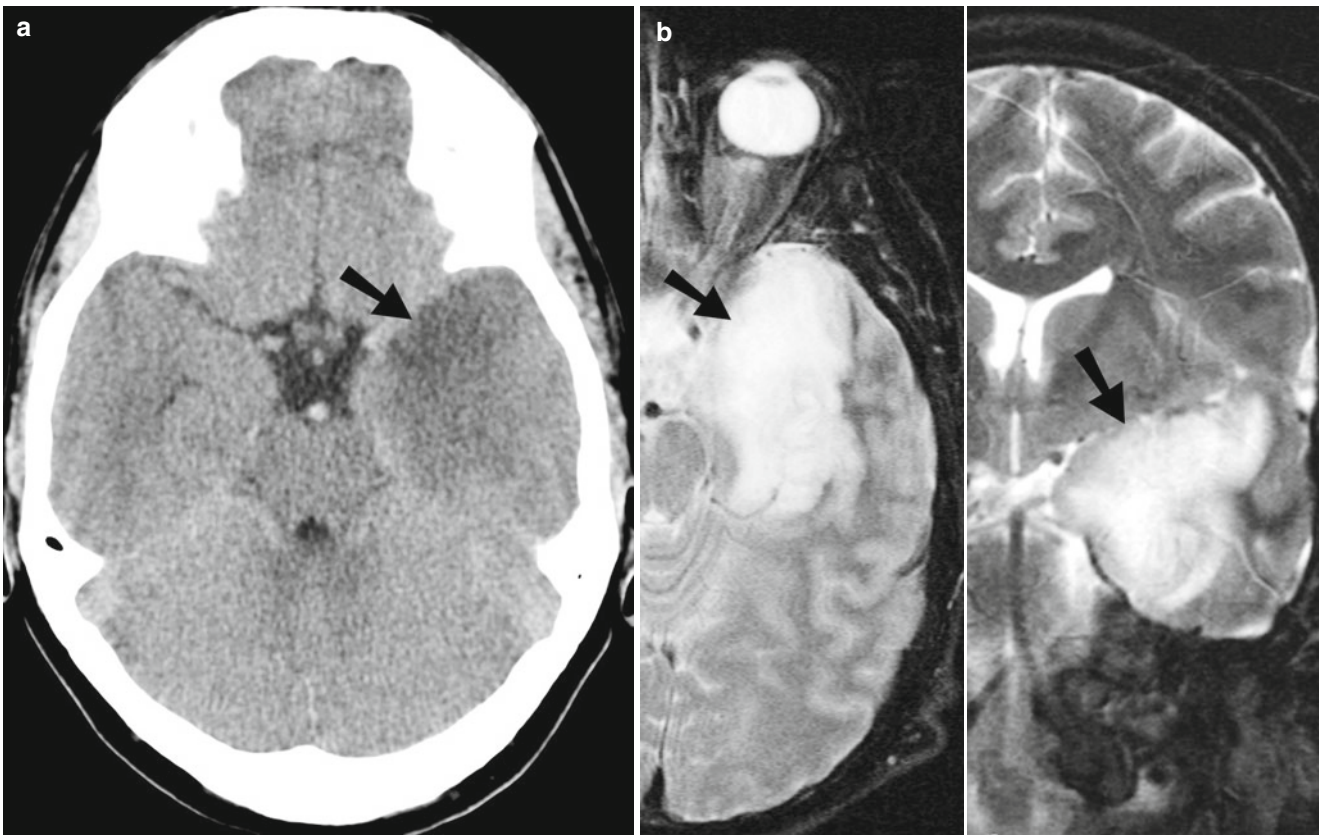

Fig. 16.4 Herpes encephalitis. (**a**) Noncontrast axial CT image of the brain shows decreased attenuation in the medial left temporal lobe (*arrow*). (**b**) Axial and coronal T2-weighted images show edema (*arrows*) in the medial temporal lobe, with contrast-enhanced T1-weighted images demonstrating patchy areas of enhancement

Tension Pneumocephalus

Tension pneumocephalus, a serious and potentially life-threatening condition, is due to increased air pressure in the subdural space causing mass effect on the frontal lobes and leading to neurological deterioration. The pathogenesis is described as a ball and valve mechanism. There is communication of the extracranial and intracranial spaces with ingress of air intracranially due to lower intracranial pressure and that the egress of air is blocked by an obstruction. Most cases occur due to head trauma but tension pneumocephalus can also occur due to skull base surgery, paranasal sinus surgery, CSF shunting, evacuation of a subdural hematoma, or posterior fossa surgery.

Patients with tension pneumocephalus often have headache and, most importantly, a diminishing level of consciousness. Imaging findings are characteristic, but not pathognomonic: prominent bifrontal subdural air collections that cause a mass effect on both frontal lobes, with widening of the interhemispheric spaces between the frontal lobes (Mt. Fuji sign) (Fig. 16.5) [5, 6].

If a patient who has had recent surgery has this imaging appearance and is clinically deteriorating, a diagnosis of tension pneumocephalus should be highly considered. Treatments include burr hole placement, craniotomy, needle aspiration, and closure of dural defects.

Giant MCA Aneurysm

Giant intracranial aneurysms are aneurysms that have a diameter greater than 2.5 cm. Most giant aneurysms are saccular rather than fusiform [7]. They tend to occur at branch points, arising de novo in defects in the intima or arising from enlarging smaller aneurysms due to hemodynamic stress. While ruptured giant aneurysms have typical symptoms of the "worst headache of my life," unruptured giant aneurysms have a sinister clinical presentation, often presenting due to mass effect on the adjacent structures or due to thromboemboli. Any large hyperdense mass in the vicinity of the cisterns and subarachnoid spaces should at least raise the possibility of a cerebral aneurysm (Fig. 16.6). Aside from

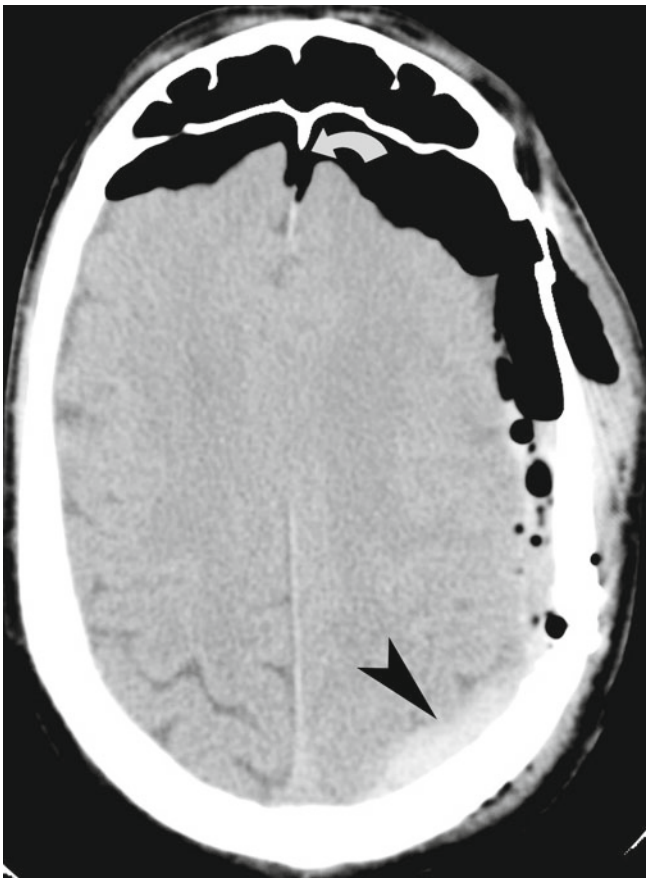

Fig. 16.5 Tension pneumocephalus. Noncontrast CT of the head shows prominent bifrontal subdural air collections with mass effect on both frontal lobes and widening of the interhemispheric space (Mt. Fuji sign) (*curved arrow*). A hyperdense left-sided subdural hematoma (*arrowhead*) is seen over the left parietal lobe

size, other imaging features of giant cerebral aneurysms are rim calcifications, a laminated and adjacent parenchymal hypodensity due to edema from pulsation.

Spontaneous Intracranial Hypotension

Spontaneous intracranial hypotension is characterized by low CSF pressure and postural headaches in the absence of prior trauma, surgery, or lumbar puncture [8]. It is usually due to an occult CSF leak from small meningeal defects. Clinical presentation is a new onset of headache with prompt and striking relief of pain in the supine position and recurrence of pain in the sitting or standing position. Headache may be associated with nausea, vomiting, vertigo, blurred vision, photophobia, neck stiffness, and occipitocervical pain with neck flexion. Imaging findings on CT or MR brain imaging include bilateral subdural hematomas, diffuse pachymeningeal enhancement, caudal displacement of the cerebellar tonsil and brainstem, decreased size of the ventricles and basal cisterns, and enlargement of the pituitary gland (Fig. 16.7) [9]. The condition is generally self-limited but treatment of associated subdural hematoma or headaches may be needed. Persistent headaches may be treated with the use of autologous epidural blood patch if conservative measures fail.

Extra-axial Hemorrhages

Extra-axial hemorrhages are classified into three main compartments: epidural, subdural, and subarachnoid (Fig. 16.8) [10].

Traumatic subarachnoid hemorrhage is the most common extra-axial hemorrhage associated with head trauma. It is caused by traumatic injuries of veins and arteries at the base of the brain, and there is less hemorrhage compared to subarachnoid hemorrhage due to aneurysm rupture.

Subdural hematomas occur between the inner dural layer and the arachnoid. Approximately half are due to shearing of the bridging veins, and the other half are due to tear of the cortical arteries. The hemorrhage is crescentic in shape acutely and crosses sutures commonly but cannot cross the midline. Interhemispheric location in children suggests non-accidental trauma.

Epidural hematomas occur in the potential space between the calvarium and the outer dural layer. The most common cause is a temporal bone fracture and arterial laceration (usually the middle meningeal artery) with smaller percentage associated with dural venous sinus tear. The hemorrhage is biconvex in configuration and is limited by sutures due to the firm adherence of the dura to the inner table and its attachment to the sutures. In less than 50 % of cases, there is a lucid interval in which the patient is knocked out by the initial concussion and then lapses into unconsciousness again after recovery. Prompt recognition and treatment can significantly decrease morbidity and mortality associated with epidural hemorrhages.

Herniation Syndromes

The brain, CSF, and blood coexist in a rigid and non-expandable container: the cranium. When most other organs enlarge, there is generally some room for expansion; however, the brain, when it expands due to edema, tumor, or hemorrhage, has very little space in which to expand. If the intracranial pressure increases enough, it will cause the brain to herniate from one compartment to another (Fig. 16.9a–d) [11].

Subfalcine herniation, the most common type of herniation, occurs when the cingulate gyrus and pericallosal branches of the anterior cerebral artery herniate beneath the falx cerebri. There is effacement of the ipsilateral ventricle and enlargement of the contralateral ventricle due to

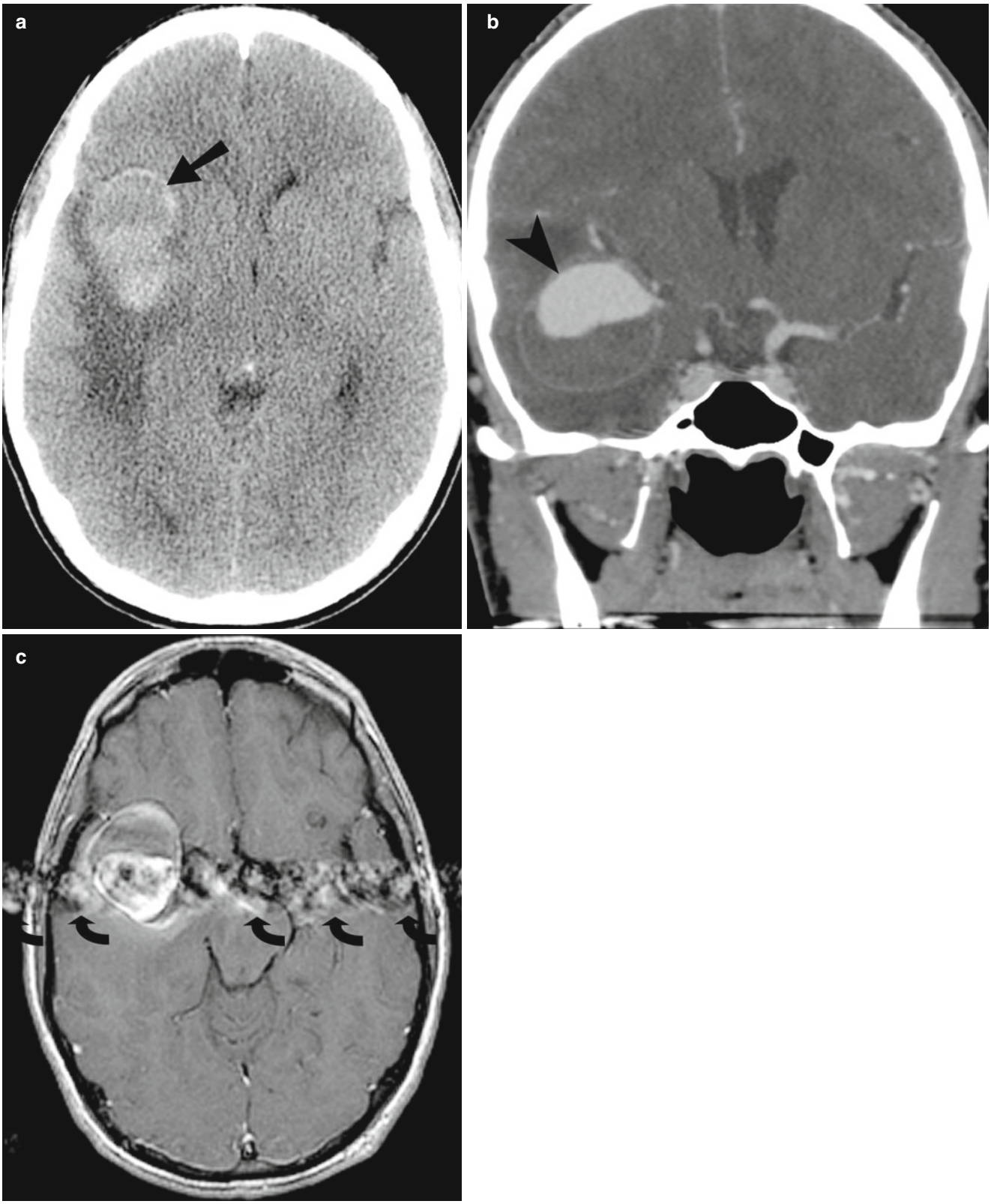

Fig. 16.6 MCA aneurysm. (**a**) Noncontrast axial CT image of the brain demonstrates a heterogeneously hyperdense lesion (*arrow*) in the right sylvian cistern with edema within the right temporal lobe. (**b**) Coronal CTA image shows a 4.5 cm diameter, partially thrombosed aneurysm (*arrowhead*) arising off the M2 segment of the right MCA. (**c**) Axial T1-weighted images with contrast show pulsation artifacts (*curved arrows*) in the phase-encoding direction, indicative of a high-flow process in the aneurysm

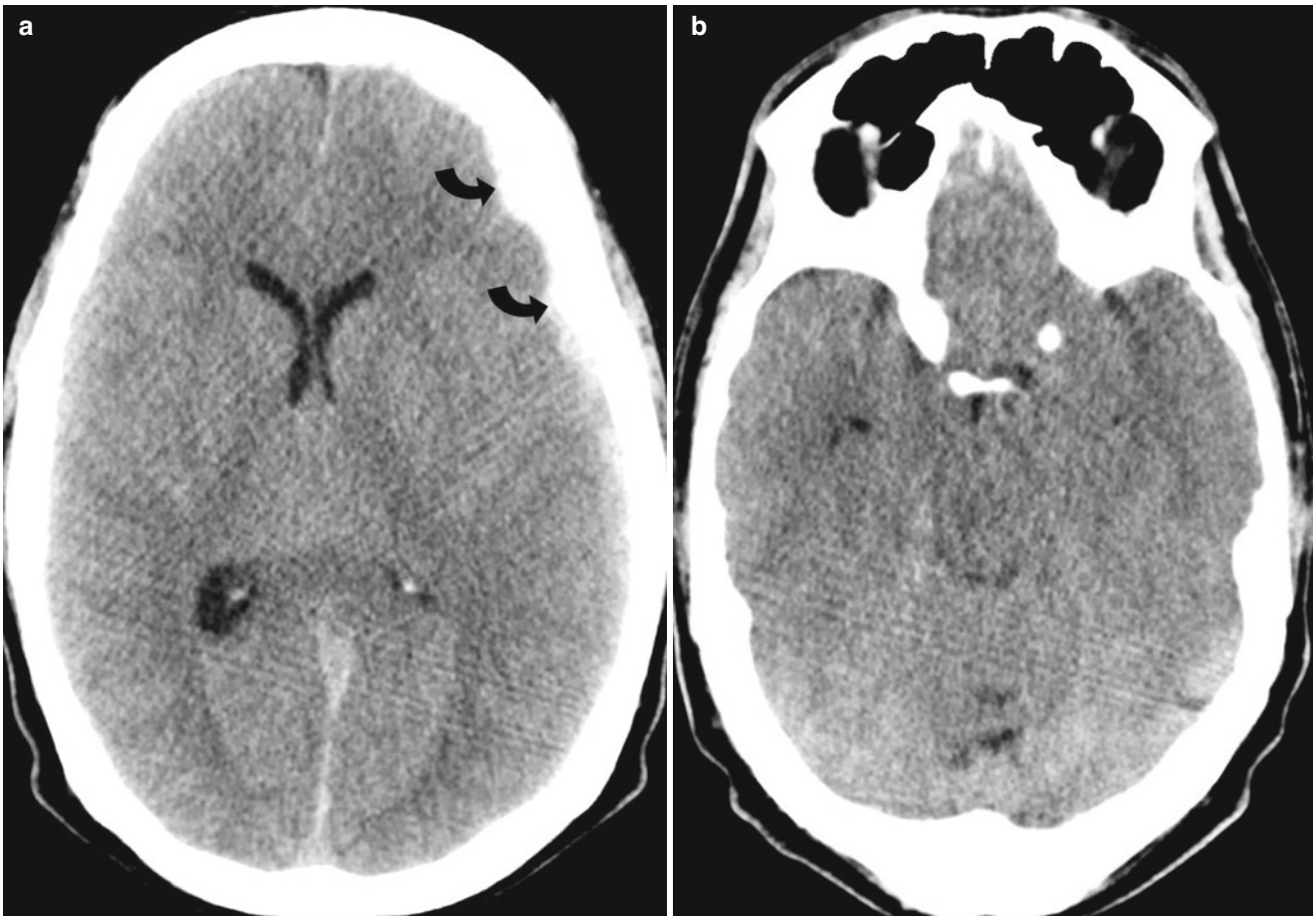

Fig. 16.7 Intracranial hypotension. (**a**) Unenhanced axial CT images of the brain demonstrate effacement of the basal cisterns, brainstem sagging, and left-sided subdural hematoma (*curved arrow*). (**b**) Unenhanced sagittal T1 MRI image of the brain demonstrates sagging of the brainstem and descent of the cerebellar tonsils

continuous production of CSF by the choroid plexus. There are possible compression of the ipsilateral anterior cerebral artery or internal cerebral veins and risk of infarction.

Uncal herniation occurs when the medial temporal lobe tissue (uncus and hippocampus) is displaced medially through the free edge of the tentorium cerebelli and compresses the brainstem and adjacent structures (posterior cerebral artery, oculomotor nerve and anterior choroidal artery). There is compression of the ipsilateral oculomotor nerve, causing a fixed and dilated pupil, and ipsilateral posterior cerebral artery, causing an infarct in its distribution. Complications also include periaqueductal necrosis; midbrain (Duret) hemorrhages; hemorrhages in the tegmentum of the pons and midbrain, as a result of stretching of the upper branches of the basilar artery; and compression of the contralateral cerebral peduncle against the free edge of the tentorium, Kernohan-Woltman notch.

Tonsillar herniation occurs due to mass effect in the posterior fossa leading to obstruction of the fourth ventricle, hydrocephalus, and inferior displacement of the cerebellar tonsils and cerebellum through the foramen magnum. There is compression of the medulla resulting in depression of the vital centers for respiration and cardiac rhythm control.

Less common herniations include central transtentorial herniation, due to end result of downward displacement of the cerebral hemispheres and basal nuclei with possible complete obliteration of the basal cisterns, and ascending transtentorial (superior vermian) herniation, caused by a slowly growing cerebellar or brainstem process forcing upward herniation of the vermis and cerebellar hemispheres through the tentorium.

Cerebral Contusions

Contusions represent acceleration/deceleration injuries to the brain involving the peripheral surfaces of the brain due to trauma. They are the second most common primary traumatic neuronal injury after diffuse axonal injury. The location of the contusions is characteristic, namely, the anterior and inferior surfaces of the temporal and frontal lobes (Fig. 16.9e, f) [12]. These parts of the brain are the

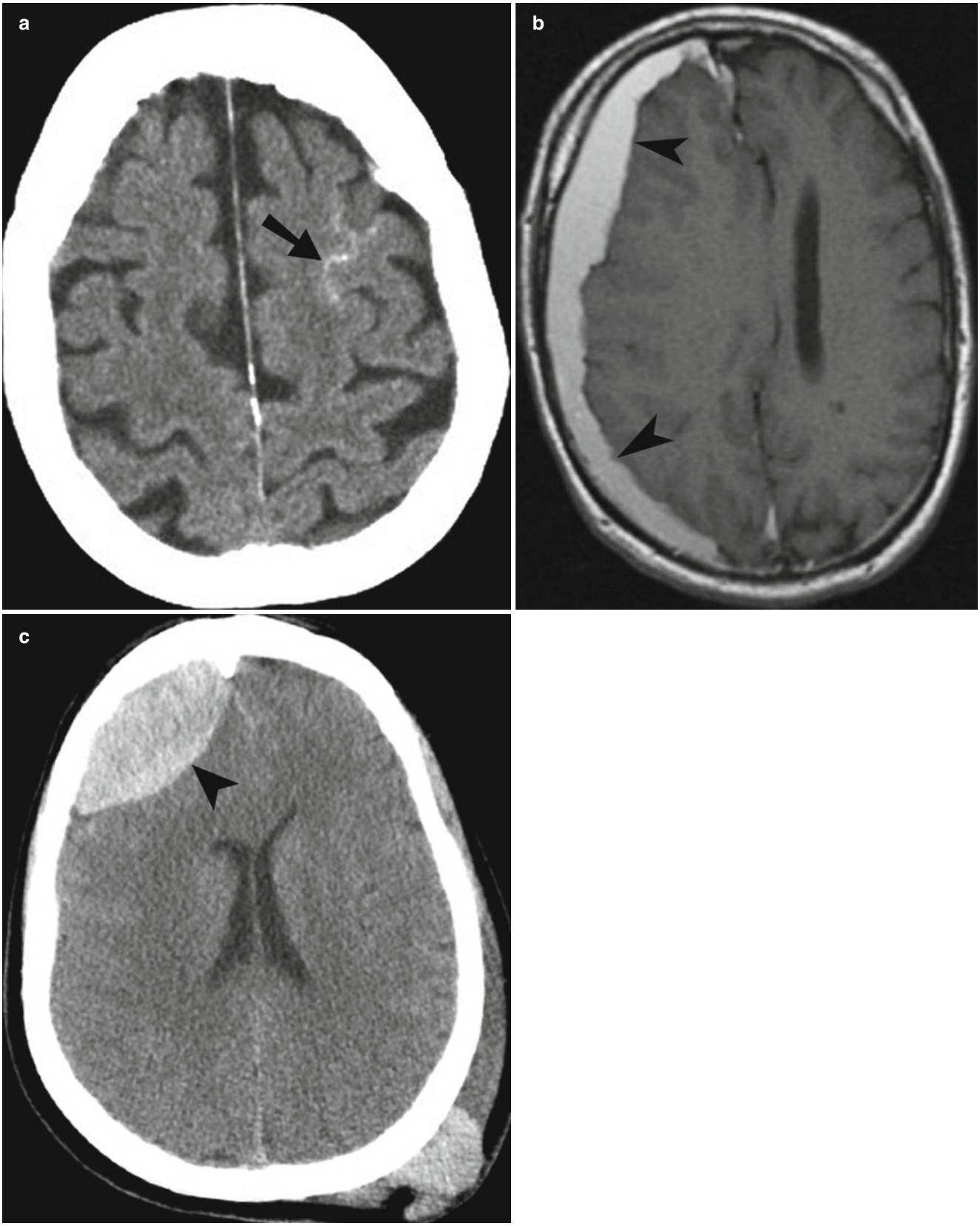

Fig. 16.8 Intracranial hemorrhage. (**a**) Noncontrast CT demonstrates subarachnoid hemorrhage (*arrow*) in the sulci over the left frontal convexity. (**b**) Unenhanced axial T1 MRI image of the brain demonstrates a hyperintense subdural fluid collection (*arrowheads*) along the right cerebral convexity consistent with a subacute subdural hematoma. (**c**) Noncontrast CT demonstrates a biconvex-shaped epidural hematoma (*arrowhead*) over the right frontal convexity produced by countercoup injury. It is producing mass effect over the right lateral ventricle

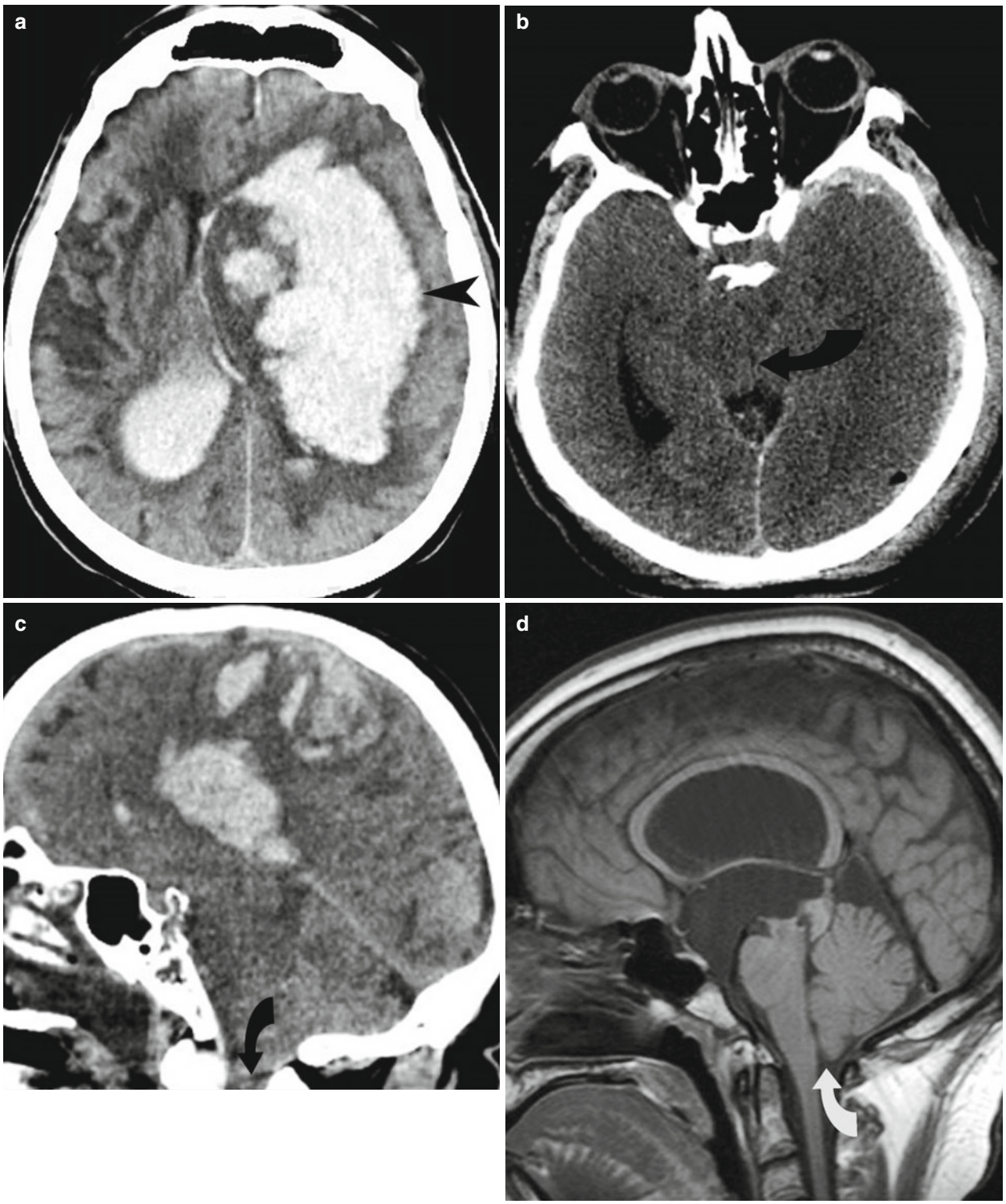

Fig. 16.9 Intraparenchymal hemorrhage. (**a**) Unenhanced axial CT image of the brain shows a large intraparenchymal hemorrhage (*arrowhead*) within the left cerebral hemisphere causing rightward subfalcine herniation. There is compression of the ipsilateral ventricle and dilatation of the contralateral ventricle and intraventricular hemorrhage. (**b**) Noncontrast CT in a patient with uncal herniation from left subdural hemorrhage demonstrates medial temporal lobe (uncus) (*curved arrow*) displaced medially through the free edge of the tentorium cerebelli and compressing the midbrain. (**c**, **d**) CT and MRI demonstrate tonsillar herniation (*curved arrows*) in two patients from parenchymal hemorrhage (**c**) and hydrocephalus (**d**). (**e**) Noncontrast axial CT images demonstrate intraparenchymal hemorrhage within the temporal and frontal lobes compatible with traumatic hemorrhagic contusions (*arrowheads*). Subarachnoid (*arrow*) and subdural blood is also seen, often coexistent with contusions. (**f**) Noncontrast CT of the head in a patient with gunshot injury demonstrates the entry wound (*arrowhead*), bullet track through the midbrain (*curved arrow*), and exit wound (*straight arrow*). There is pneumocephalus as well as subarachnoid hemorrhage

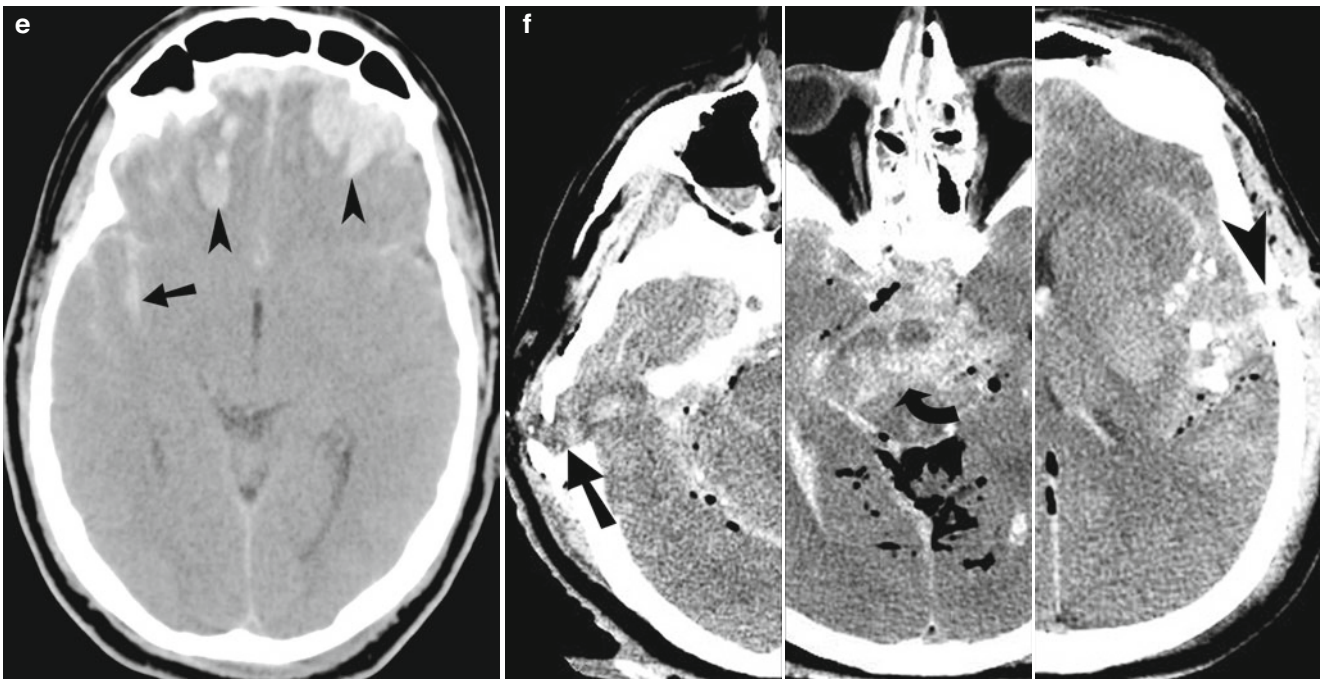

Fig. 16..9 (continued)

most mobile areas and have more fixed proximal portions and thus brush up against the irregular inner calvarial surfaces of the anterior and inferior frontal bone of the anterior cranial fossa and the greater sphenoid wing and temporal bone in the middle cranial fossa. Less frequently, contusions can occur in the parasagittal cerebral hemispheres, as the parenchyma contuses along the rigid interhemispheric falx.

It is important in the setting of contusions, both hemorrhagic and nonhemorrhagic, to get short-term follow-up, as new lesions may appear within the first few days, and existing injuries may become larger. An important differential to exclude is venous occlusive disease, as sinus thrombosis can often have a similar appearance and location. The treatment is to prevent secondary injury, such as hematoma formation, mass effect, or herniation – all or which may require surgical intervention.

Cortical Laminar Necrosis

Cortical laminar necrosis is important to know for two reasons: one, it is a hallmark of subacute injury, i.e., roughly 14–21 days after initial insult; two, the cortical hyperdensity (or hyperintensity on T1 MRI) is secondary to *hypoxic* ischemic injury rather than hemorrhagic injury. This patient was a 35-year-old female who earlier had a cesarean section and, approximately 3 months postpartum, presented to the emergency department with signs and symptoms of hypertensive urgency. The patient's labile response to blood pressure correction led to a severe pressure drop, which precipitated worsening mental status changes. Subsequent head CT exams demonstrated patchy hypodensities in the parietal and occipital lobes. Three weeks after presentation, findings had progressed to laminar necrosis.

The differential diagnosis includes cerebritis, low-grade cortical neoplasm, and Sturge-Weber. Hyperdense gyri may or may not be present on CT, but the characteristic high signal intensity on T1 sequence is most sensitive (Fig. 16.10) [13]. Subacute infarcts are infrequently imaged, and so knowledge of the myriad imaging appearances, coupled with appropriate history, can often aid clinicians in treatment and prevent needless tests (i.e., neoplasm or infectious disease workups).

Overall, the presence of cortical laminar necrosis is indicative of a poor clinical prognosis. Interestingly, although incompletely understood, the hyperdensity and hyperintensity on CT and MRI are not due to blood or calcification, but felt to be due to reactive gliosis and fat-laden macrophages. To our knowledge, there is no association in the literature between CLN and hypertension or hypertensive crisis.

Cerebral Arterial Air Embolism

Aside from the airway, the paranasal sinuses, and the mastoid and petrous temporal bones, the head should not have air within it. Cerebral air emboli can be venous or arterial.

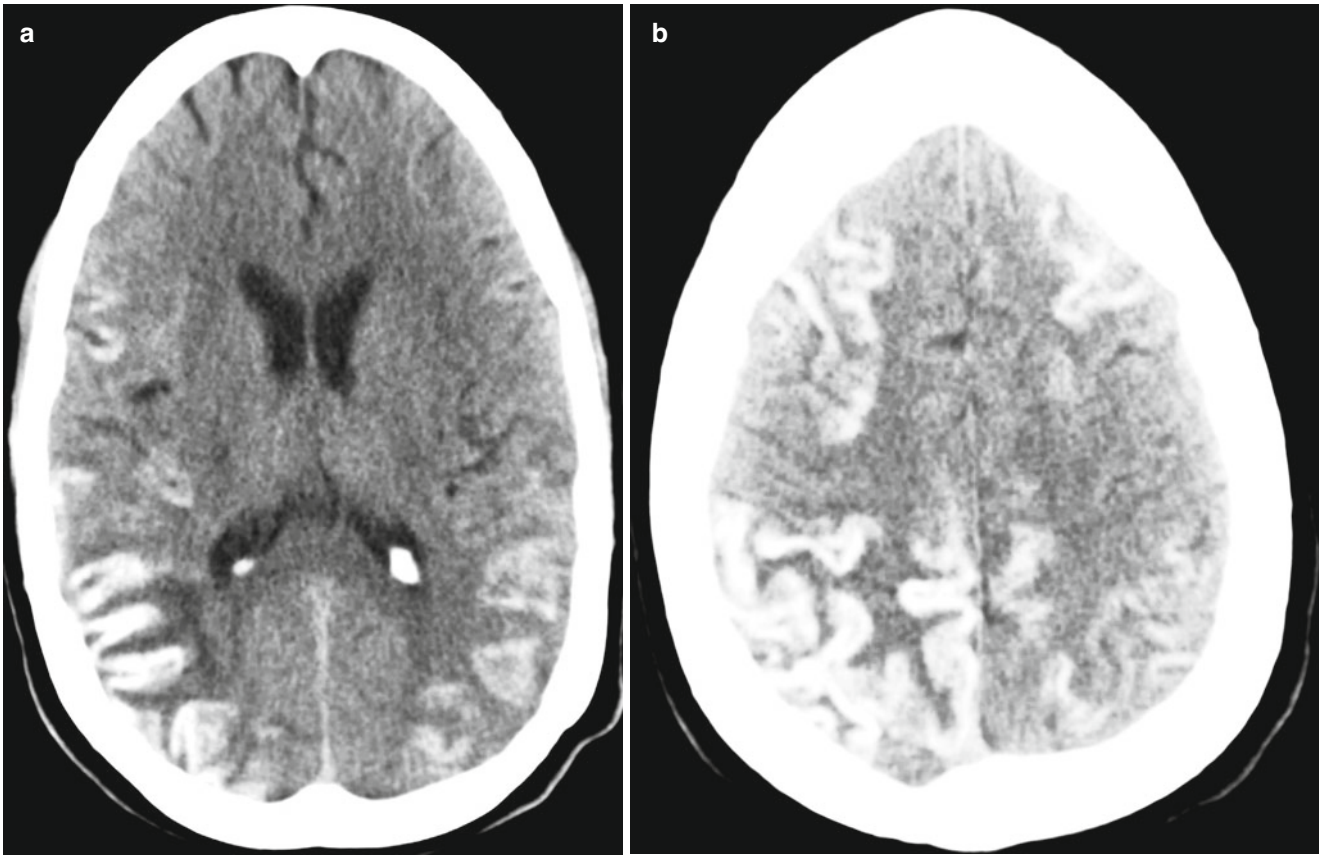

Fig. 16.10 Cortical laminar necrosis. (**a**, **b**) Noncontrast axial CT images of the brain demonstrate extensive, diffuse cortical gyral wavy hyperdensities, most consistent with cortical laminar necrosis. Although incompletely understood, the hyperdensity and hyperintensity on CT are not due to blood or calcification

Venous air emboli can occur due to central catheter placement or other instrumentation related to venous access such as from a CT injector. Intracranially, air is often seen in the cavernous sinus and superficial maxillofacial venous branches. If minimal, patients are often asymptomatic, but it is still worthwhile to alert the clinicians of the presence of venous air.

Arterial cerebral air embolism, however, is an infrequent but potentially devastating entity with serious sequelae. Arterial air emboli can cause an inflammatory response that can result from the air itself or due to a reduction in perfusion distal to the obstruction [14].

Arterial air emboli are often the result of trauma, surgery, or procedures such as lung biopsy. Air can reach the arterial system through the pulmonary vein (and ultimately the systemic circulation) via a biopsy needle or broncho-venous fistula of any cause, by way of the systemic venous side by traversing the pulmonary microvasculature (even without an arteriovenous communication) or through any form of right-to-left shunt. The air detected on CT scan can reabsorb rapidly and therefore will not be apparent on a follow-up study (Fig. 16.11).

Patients often present with generalized seizures and focal neurological deficits. Treatment is 100 % oxygen, aggressive fluid resuscitation, and hyperbaric oxygen therapy. Prompt diagnosis and clinician communication can initiate aggressive treatment and mitigate the extent of damage.

Obstructive Hydrocephalus

Obstructive hydrocephalus is caused by obstruction to the flow of CSF at the level of foramen of Monro, third ventricle, aqueduct of Sylvius, or fourth ventricle. The imaging findings of obstructive hydrocephalus include prominence of ventricular system above the occlusion. The most common site of obstruction is aqueduct of Sylvius and results in prominence of the lateral and third ventricle. Obstruction to the outflow of the fourth ventricle results in additional prominence of the fourth ventricle which loses its triangular configuration and appears round. The supratentorial cisterns, fissures, and sulci are much less prominent due to ventricular dilatation. Periventricular edema may occur due to transependymal spread of fluid (Fig. 16.12).

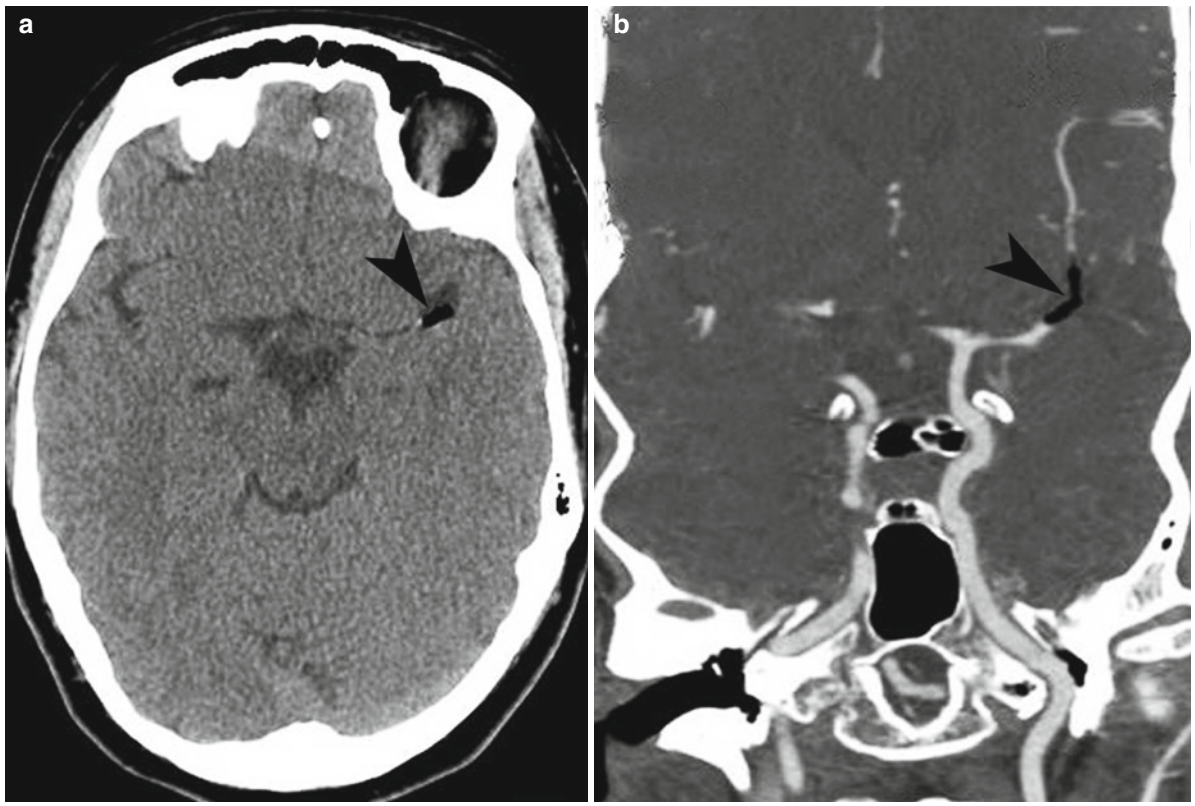

Fig. 16.11 Air embolism. (**a**, **b**) Noncontrast axial CT and CT angiogram of the brain demonstrate a focal area of intravascular air (*arrowhead*) within the M1 (sylvian) segment of the left middle cerebral artery, compatible with arterial air embolism

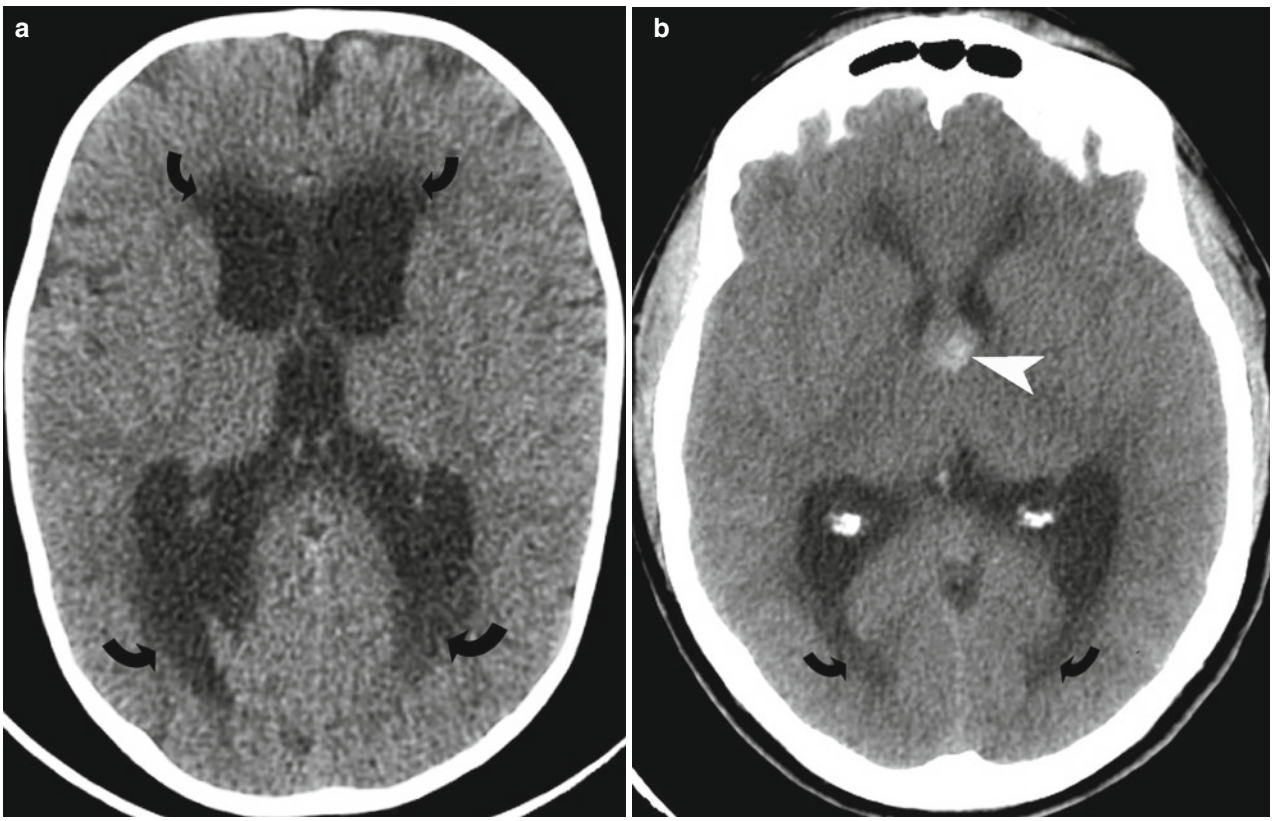

Fig. 16.12 Obstructive hydrocephalus. (**a**, **b**) Noncontrast CT of the head demonstrates acute obstructive hydrocephalus with transependymal edema (*curved arrows*), caused by posterior fossa hemorrhage (**a**) and colloid cyst at the foramen of Monro (*arrowhead*) (**b**). (**c**) T2-weighted MRI shows acute obstructive hydrocephalus with transependymal edema (*curved arrows*) around the lateral ventricles

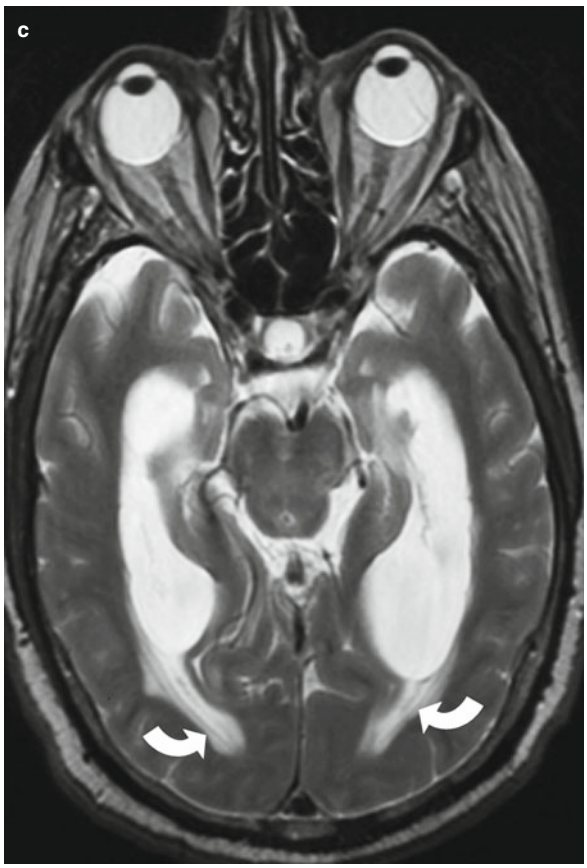

Fig. 16.12 (continued)

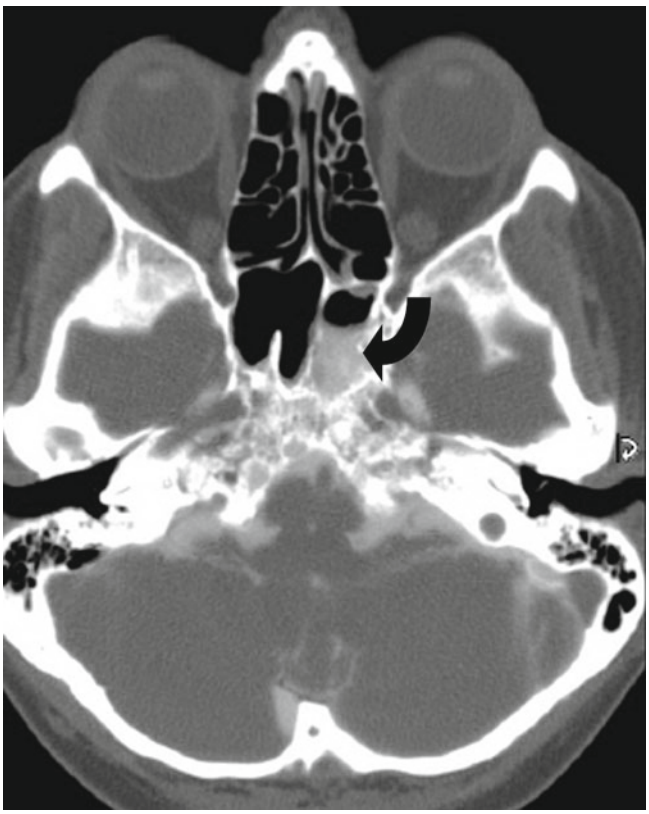

Fig. 16.14 Posttraumatic CSF leak. CT cisternogram study demonstrates radiopaque contrast leaking through dural and osseous defect in sphenoid sinus wall. The contrast is seen collecting in the left sphenoid sinus (*curved arrow*)

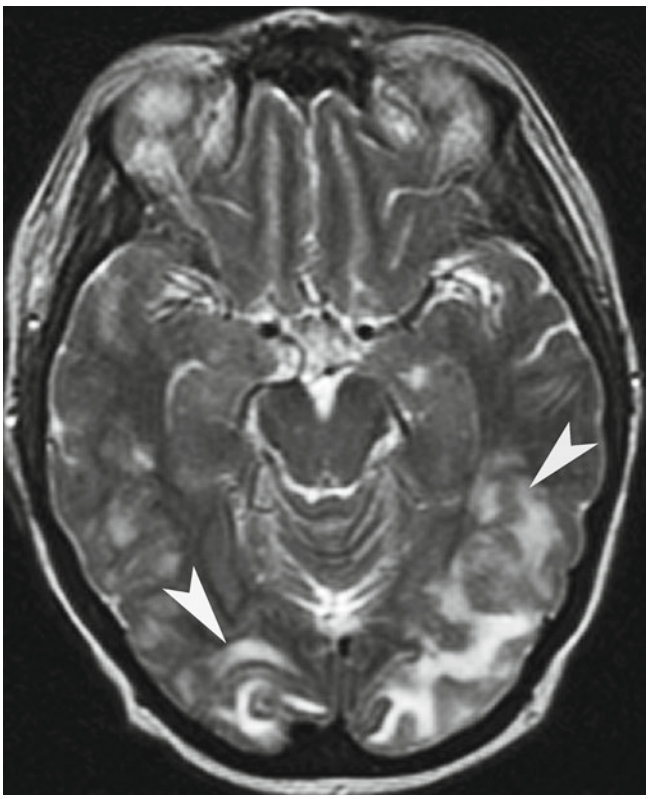

Fig. 16.13 Acute hypertensive encephalopathy. T2-weighted MR image demonstrates patchy and confluent hyperintensities (*arrowheads*) in both occipital lobes

Acute Hypertensive Encephalopathy

It is seen in patients with severe hypertension and is believed to be due to abnormal cerebrovascular autoregulation. It is also called posterior reversible encephalopathy syndrome.

On CT imaging, there is bilateral cortical or subcortical low density, most commonly in the posterior circulation. The occipital lobes and posterior parietal lobes are most commonly involved by the process, which is more often patchy than confluent (Fig. 16.13). On MR imaging, the patchy lesions are bright on T2-weighted and FLAIR sequences. The differential diagnosis includes cerebral infarcts, progressive multifocal encephalopathy, demyelinating disease, and metabolic derangements (dialysis).

CSF Leak

Majority (90 %) of the cases are posttraumatic, often occurring through the floor of anterior cranial fossa and resulting in CSF rhinorrhea. Fracture of temporal bone may result in otorrhea, accounting for 20 % of the cases. Eighty percent of CSF leak occur within 48 h for the traumatic event and 95 % occur within 3 months.

CT cisternogram is the gold standard in demonstrating CSF leak from the base of skull. If the CSF leak is intermittent,

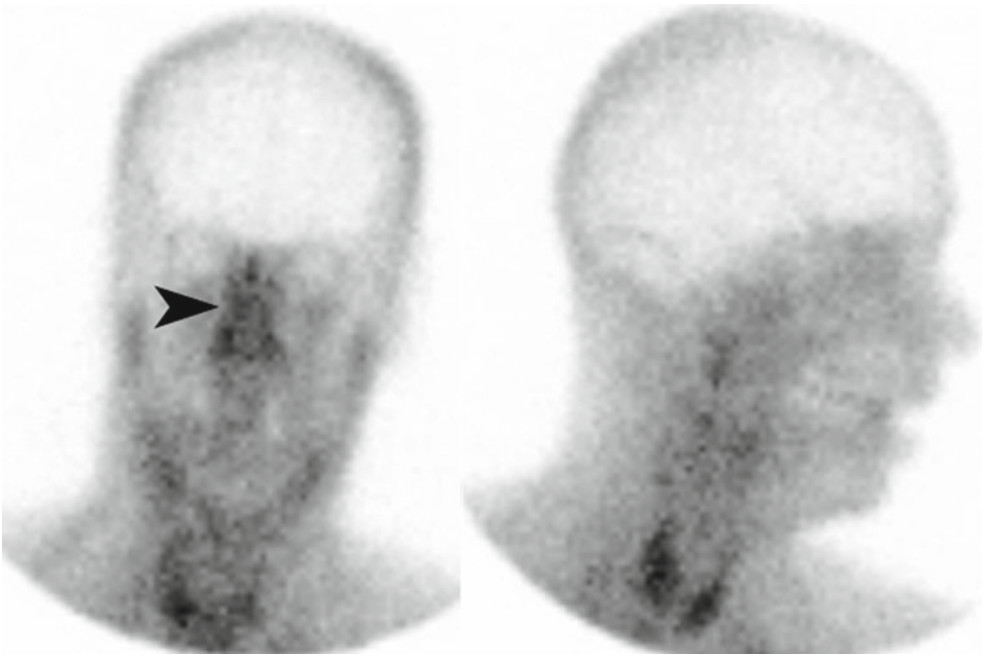

Fig. 16.15 Brain death. Tc99m HMPAO study demonstrates hot nose sign (*arrowhead*) in this patient with no intracranial uptake (light bulb sign) of radiotracer

then the timing of the study is important in detecting the leak. A positive study will show contrast material leaking through the dural and osseous defect (Fig. 16.14). Since the anatomical site of defect is more difficult to see on radionuclide cisternograms (indium 111 diethylenetriaminepentaacetic acid), they are used as second-line imaging modality. The biological half-life of 2.8 days prolonged imaging for up to 3 days after radiotracer administration.

Brain Death

The best imaging test to confirm brain death is a neuralite study. Brain death is characterized by irreversible loss of brain function with marked brain swelling and obliteration of sulci. The intracranial pressure exceeds the vascular perfusion pressure and leads to irreversible ischemia. The EEG of a patient with brain death is isoelectric due to cessation of physiologic functions.

Normal brain shows uptake of Tc99m HMPAO, and Tc99m ECD does cross the blood–brain barrier, in proportion to the regional blood flow. On Tc99m ECD (neuralite) or Tc99m HMPAO (Ceretec) study, there is no flow to the intracranial supratentorial as well as infratentorial structures after brain death. These patients will typically show increased radiotracer in the nasal area (hot nose sign). The absence to radiotracer in the intracranial region produces a lightbulb sign (Fig. 16.15).

References

1. Given CA et al. Pseudo-subarachnoid hemorrhage: a potential imaging pitfall associated with diffuse cerebral edema. AJNR Am J Neuroradiol. 2003;24:254–6.
2. Sener RN. Acute carbon monoxide poisoning: diffusion MR imaging findings. AJNR Am J Neuroradiol. 2003;24:1475–7.
3. Paolini S et al. Gas-containing otogenic brain abscess. Surg Neurol. 2002;58(3–4):271–3.
4. Baringer JR. Herpes simplex infections of the nervous systems. Neurol Clin. 2008;26(3):657–74, viii.
5. Sinclair AG et al. Imaging of the post-operative cranium. Radiographics. 2010;30:461–82.
6. Michel SJ. The Mount Fuji sign. Radiology. 2004;232:449–50.
7. Mehta RI et al. Best cases from the AFIP: giant intracranial aneurysm. Radiographics. 2010;30:1133–8.
8. Jacobs MB, Wasserstein PH. Spontaneous intracranial hypotension: an uncommon and underrecognized cause of headache. West J Med. 1991;155:178–80.
9. Watanabe A, Horikoshi T, Uchida M, Koizumi H, Yagishita T, Kinouchi H. Diagnostic value of spinal MR imaging in spontaneous intracranial hypotension syndrome. AJNR Am J Neuroradiol. 2009;30:147–51.
10. Osborn AG, Salzman KL, Barkovich J. Trauma. In: Diagnostic imaging brain. 2nd ed. London: Amirys Publishing, Inc; 2005. p. I-2-3.
11. Coburn MW, Rodriguez FJ. Cerebral herniations. Appl Radiol. 1998;27:10–6.
12. Kim JJ et al. Imaging for the diagnosis and management of traumatic brain injury. Neurotherapeutics. 2011;8(1):39–53.
13. Kinoshita T et al. Curvilinear T1 hyperintense lesions representing cortical necrosis after cerebral infarction. Neuroradiology. 2005;47:647–51.
14. Yang MS et al. Iatrogenic and fatal air arterial embolism during CT scan. J Chin Med Assoc. 2011;74:188–91.